Published in final edited form as:
Nat Neurosci. 2014 October ; 17(10): 1330–1339. doi:10.1038/nn.3808.

Genome-wide identification and characterization of functional neuronal activity-dependent enhancers

Athar N. Malik[1,2,3,*], **Thomas Vierbuchen**[1,*], **Martin Hemberg**[4], **Alex A. Rubin**[1], **Emi Ling**[1,5], **Cameron H. Couch**[1], **Hume Stroud**[1], **Ivo Spiegel**[1], **Kyle Kai-How Farh**[1,6], **David A. Harmin**[1], and **Michael E. Greenberg**[1,#]

[1]Department of Neurobiology, Harvard Medical School, 220 Longwood Avenue, Boston, Massachusetts , USA

[2]M.D.-Ph.D. Program, Harvard Medical School, 260 Longwood Avenue, Boston, Massachusetts, USA

[3] Division of Health Sciences and Technology, Harvard Medical School and Massachusetts Institute of Technology, 77 Massachusetts Avenue, Cambridge, Massachusetts, USA

[4]Department of Ophthalmology, Children's Hospital Boston, Harvard University, 300 Longwood Avenue, Boston, Massachusetts, USA

[5]Program in Biological and Biomedical Sciences, Harvard Medical School, 25 Shattuck Street, Boston, Massachusetts, USA

[6]Broad Institute of MIT and Harvard, Cambridge, Massachusetts, USA

SUMMARY

[#]Correspondence should be addressed to: M.E.G. (Michael_Greenberg@hms.harvard.edu).
[*]Shared first authorship

Supplementary methods checklist: A supplementary method checklist is available with the online materials.

Accession codes: The ChIP-seq data generated in this study, including relevant processed data files, have been deposited onto GEO under accession number GSE60192. The microarray gene expression data generated in this study, including relevant processed data files, have been deposited onto GEO under accession number GSE60049.

Referenced accession codes:
GSE21161
GSE52386
Forebrain E11.5 H3K27ac Rep1 (GSM1264352)
Forebrain E11.5 H3K27ac Rep2 (GSM1264354)
Forebrain E14.5 H3K27ac (GSM1264356)
Forebrain E17.5 H3K27ac (GSM1264358)
Forebrain P0 H3K27ac (GSM1264360)
Forebrain P7 H3K27ac (GSM1264362)
Forebrain P21 H3K27ac (GSM1264364)
Forebrain P56 H3K27ac Rep1 (GSM1264366)
Forebrain P56 H3K27ac Rep2 (GSM1264368)

Author contributions: A.N.M. and M.E.G. conceived the study. A.N.M. performed experiments with assistance from T.V., A.A.R., E.L., I.S. and C.C. A.N.M. performed analysis of microarray experiments. A.N.M. performed analysis of genome-wide sequencing experiments with assistance from M.H, H.S., K.K.H.F. and D.A.H. A.N.M generated figures with assistance from T.V. T.V., A.N.M. and M.E.G. wrote the manuscript.

Competing financial interests statement: The authors declare no competing financial interests.

Experience-dependent gene transcription is required for nervous system development and function. However, the DNA regulatory elements that control this program of gene expression are not well defined. Here we characterize the enhancers that function across the genome to mediate activity-dependent transcription in mouse cortical neurons. We find that the subset of enhancers enriched for monomethylation of histone H3 lysine 4 (H3K4me1) and binding of the transcriptional co-activator CREBBP (CBP) that shows increased acetylation of histone H3 lysine 27 (H3K27ac) upon membrane depolarization of cortical neurons functions to regulate activity-dependent transcription. A subset of these enhancers appears to require binding of FOS, which previously was thought to bind primarily to promoters. These findings suggest that FOS functions at enhancers to control activity-dependent gene programs that are critical for nervous system function and provide a resource of functional *cis*-regulatory elements that may give insight into the genetic variants that contribute to brain development and disease.

INTRODUCTION

In the nervous system, sensory experience promotes both the refinement and maturation of synaptic connections and the subsequent modification of neural circuits during learning, memory, and behavior[1–6]. Sensory experiences produce long-lasting changes in neuronal function in part through activity-dependent gene expression. In response to sensory input, synaptic activity leads to membrane depolarization of the post-synaptic neuron, triggering calcium influx through L-type voltage-gated calcium channels. This leads to the activation of a complex signaling network that alters the post-translational modification of transcription factors (e.g. MEF2, CREB, SRF), transcriptional co-factors (e.g. CBP), and chromatin modifiers (e.g. HDACs, MECP2) resulting in the transcription of early-response genes[1,6]. Many early-response genes encode transcription factors (e. g. FOS, FOSB, JUNB, EGR1, NR4A1, and NPAS4) that control the expression of late-response genes (e.g., *Bdnf*, *Nptx2*) that regulate diverse aspects of nervous system development and function, including dendritic development, synapse maturation, synaptic plasticity, and learning and memory[2,7–9]. In total, several hundred neuronal activity-regulated genes have been identified, suggesting that activation of this gene expression program could broadly modify neuronal function. Furthermore, mutations in components of the neuronal activity-dependent transcriptional program have been linked to human cognitive disorders, including intellectual disability, autism spectrum disorders and psychiatric illness[10]. This has heightened interest in defining the functions of the components of the activity-dependent signaling network in specific neuronal subtypes in the developing and mature nervous system.

There is still a striking gap in our understanding of how early-response transcription factors such as FOS, C-JUN, NR4A1, and EGR1 function to promote the transcription of late-response genes[1,2,4]. Although these transcription factors are activated in virtually every mammalian cell in response to extra-cellular stimuli, it remains to be determined at a genome-wide level if activity-induced transcription factors actually bind to gene promoters in neurons, and if so how they facilitate transcriptional initiation. The best characterized of the early-response transcription factors is FOS[11–13]. Reporter gene and DNA mobility shift assays have demonstrated that FOS binds as a heterodimer with JUN family members to the

AP-1 motif (TGANTCA) within the promoters of stimulus-responsive genes and thereby stimulates late-response gene transcription[13]. However, it was not known where FOS complexes bind across the genome in stimulated neurons, if in fact FOS is a promoter-binding factor, and the extent of the gene network activated by FOS in response to neuronal activity. In addition, the possibility that FOS binds to regulatory sequences other than promoters, such as enhancers, had not been broadly explored.

Enhancers are regulatory sequences that typically reside long distances from promoters yet are able to effectively boost gene transcription[14,15]. The advent of next generation sequencing technologies such as chromatin immunoprecipitation paired with high-throughput sequencing (ChIP-seq) and genome-wide transcriptomics (RNA-seq) have facilitated identification of enhancer sequences at a genome-wide level[16–18]. An emerging view is that enhancers bind transcription factors and enable spatiotemporal control of tissue-specific gene expression during development. In addition, enhancers are increasingly appreciated to be the sites of functional variation within the genome that contribute to human disease[19]. Thus, there is significant interest in identifying enhancers that regulate nervous system development and function[20,21]. A key step towards this end will be to identify the enhancers that control activity-dependent gene transcription.

Chromatin and transcription factor signatures have been identified that enable the unbiased genome-wide detection of enhancers. For example, enhancers have been identified as sequences where H3K4me1 is enriched and transcriptional co-activators such as CBP or EP300 (p300) are bound[16,17]. Building upon these findings, a recent study measured CBP binding before and after membrane depolarization in cortical neurons to identify neuronal activity-dependent enhancers[18]. Although nearly 12,000 H3K4me1 enriched genomic regions exhibited activity-dependent increases in CBP binding, this far exceeds the number of activity-regulated genes, suggesting that many of these enhancers might not function to promote activity-regulated transcription. Consistent with this possibility, several recent studies in non-neuronal cells have shown that only the subset of CBP/p300-bound enhancers that exhibit acetylation of H3K27ac are actively engaged in regulating transcription[22,23]. These data suggested that the presence of the H3K27ac signature might mark enhancers that are functionally engaged in regulating gene transcription.

It is not known which of the thousands of putative activity-regulated enhancers in neurons contribute to activity-dependent transcription or if the H3K27ac mark is relevant to the function of these enhancers[24]. One possibility is that the subset of the activity-regulated CBP binding sites that function as activity-dependent enhancers display an increase in H3K27ac in response to stimuli that induce activity-dependent gene transcription. If this increase in H3K27ac is tightly correlated with enhancer activation, it might be used to help identify the functionally relevant activity-dependent enhancers. Alternatively, a subset of CBP binding sites might have the H3K27ac signature prior to activation, facilitating subsequent events that are required for enhancer activation.

To distinguish between these possibilities we performed ChIP-seq to assess the level of H3K27ac at enhancers before and after membrane depolarization of cultured cortical neurons. We found that neuronal activity induces an increase in H3K27ac at only a small

subset of the ~12,000 CBP binding sites in neurons, but that the presence of increased H3K27ac predicts with 100% accuracy the enhancers that are capable of stimulating activity-dependent gene transcription. Surprisingly, a large proportion of these activity-regulated enhancers bind FOS. We find that FOS binds almost exclusively to enhancers and mediates the neuronal response to activity by amplifying the transcription of a wide range of activity-regulated genes that control synaptic function.

In this study, we identify the subset of activity-regulated enhancers that control gene transcription in cultured cortical neurons and that appear to be active *in vivo* during the postnatal period when experience-dependent gene transcription regulates synaptic maturation. In addition, we find that FOS, a protein that was thought to bind primarily to gene promoters, functions almost exclusively at enhancers to mediate the neuronal transcriptional response to elevated levels of activity. Since many of these FOS-bound enhancer elements are active in the developing post-natal brain, they are potentially sites of sequence variation that may underlie differences in human brain function, and whose mutation could give rise to nervous system disorders.

Neuronal activity-regulated H3K27ac dynamics at enhancers

To clarify which of the ~12,000 previously characterized activity-regulated enhancers (i.e. those that exhibit enrichment of H3K4me1 and inducible binding of CBP, termed CBP/H3K4me1-enriched enhancers) function to promote activity-dependent transcription, we used ChIP-seq to assess H3K27ac across the genome in mouse cortical neurons before and after their exposure to elevated levels of KCl (55 mM). This treatment has previously been shown to lead to membrane depolarization and an influx of calcium into neurons via L-type voltage sensitive calcium channels. The elevation in intra-cellular calcium then triggers activity-dependent gene transcription. A large number of studies have shown that membrane depolarization of cultured neurons with elevated levels of KCl is a valid way of identifying signaling network components that function in the intact brain to mediate the genomic response to a wide range of sensory stimuli[1,18].

We hypothesized that membrane depolarization might lead to the induction of H3K27ac at enhancers, which might be a key step in enhancer activation. To test this idea we initially focused our attention on enhancers within the *Fos* locus. Activity-dependent induction of *Fos* transcription had been suggested to be mediated by five CBP/H3K4me1-enriched enhancers[18]. These putative *Fos* enhancers lie within 35kb of the initiation site of *Fos* mRNA synthesis. We found that compared to untreated cells, exposure of cortical neurons to 55 mM KCl for two hours leads to a significant increase in H3K27ac and CBP binding at the *Fos* promoter and at four of the five *Fos* enhancers described previously (Fig. 1a)[18]. This increase in H3K27ac correlates with a large increase in the production of *Fos* mRNA raising the possibility that the activity-dependent increase in H3K27ac at the *Fos* enhancers might be required for enhancer activation and *Fos* transcription.

If the induction of H3K27ac at an enhancer is required for activity-dependent enhancer activation then the induction of this modification at enhancers might be used to determine which among the thousands of putative enhancers are functionally engaged in driving activity-dependent transcription. To investigate this, we first identified H3K27ac peaks

genome-wide before and after membrane depolarization. H3K27ac ChIP-seq signal was highly reproducible between biological replicates (Spearman's ρ=0.91, ρ=0.94 for unstimulated and membrane-depolarized replicates; Supplementary Fig. 1a–b). We filtered out peaks that were located within 1 kb of an annotated TSS, which likely represent promoters (Fig. 1b–c). Among these distal H3K27ac peaks, there were numerous peaks that were detected only after membrane depolarization (n = 4902; Fig. 1c), suggesting that the genome-wide distribution of H3K27ac was modified by membrane depolarization. Both before and after membrane depolarization, these distal H3K27ac sites were enriched for the enhancer-associated histone modification H3K4me1 and had low levels of both H3K4me3 (associated with promoters) and H3K27me3 (associated with polycomb-mediated gene silencing) (Fig. 1d). Interestingly, we observed that H3K27ac levels change in response to neuronal activity at putative enhancers throughout the genome much more than H3K4me1 levels (Spearman's ρ = 0.79 vs. ρ = 0.96; Fig. 2a–b and Supplementary Fig. 1c–d), suggesting that changes in H3K27ac may reflect changes in enhancer function in response to neuronal activity. As a first step towards determining if increased H3K27ac could be used to identify the CBP/H3K4me1-enriched sites across the genome that function as enhancers, we searched for CBP/H3K4me1-enriched sites with an increase in H3K27ac in response to membrane depolarization. Genome-wide quantification of H3K27ac levels at putative activity-regulated enhancers (CBP/H3K4me1-enriched >1kb from an annotated TSS; see methods) revealed that in response to membrane depolarization, a relatively small subset of these sites (n = 1468, ~12%) exhibit at least a two-fold increase in H3K27 acetylation (Increasing H3K27ac; Fig. 2c–d). Some putative activity-regulated enhancers exhibited a high level of H3K27ac prior to stimulation that remained unchanged upon membrane depolarization (Constant H3K27ac), whereas other CBP binding sites displayed a low level of H3K27ac both before and after stimulation (No H3K27ac; Fig. 2c–d). We also identified sites that undergo a decrease in H3K27ac in response to membrane depolarization (Decreasing H3K27ac; Fig. 2c–d). Membrane depolarization induced changes in the level of H3K27ac at gene distal sites also occurred where CBP/H3K4me1 enrichment was not detected (Supplementary Fig. 1c–e).

We divided each of the putative regulatory elements with CBP/H3K4me1-enrichment into four categories based on their relative level of H3K27ac before and after membrane depolarization: those with increasing, constant, decreasing, or no H3K27ac in response to stimulation (Fig. 2c–d). To determine if the H3K27ac status of a putative activity-regulated enhancer can identify whether the enhancer is capable of stimulating activity-dependent transcription we measured the ability of sites from each category to stimulate activity-dependent transcription. For this purpose we developed a neuronal activity-regulated luciferase reporter gene in which 4kb of the regulatory region of the activity-regulated gene neuronal pentraxin 2 (*Nptx2*), including the *Nptx2* TSS, was cloned 5' to the luciferase gene (see methods)[25]. The cloned *Nptx2* regulatory region includes an enhancer that is located ~3 kb upstream of the *Nptx2* TSS that we found to be critical for activity-dependent induction of reporter gene expression (Fig. 3a). To determine if CBP/H3K4me1-enriched loci exhibiting activity-dependent increases in H3K27ac were capable of inducing activity-driven reporter gene transcription, we replaced the *Nptx2* upstream enhancer with 14 different enhancers with increasing H3K27ac enhancers and measured luciferase expression

before and after membrane depolarization. Strikingly, we found that 100% (14/14) of these enhancers drove robust activity-dependent transcription of the luciferase reporter gene (2.44×10^{-5}; Students t-test, two-tailed; Fig. 3a and Supplementary Fig. 2a). By contrast, CBP/H3K4me1-enriched loci that displayed constant levels of H3K27ac before and after stimulation or exhibited no H3K27ac either before or after stimulation were not effective at inducing activity-dependent transcription of the luciferase reporter gene (p = 0.206, 0.422; Student's t-test, two-tailed). Regulatory sequences with CBP/H3K4me1-enrichment and a reduction in H3K27ac upon membrane depolarization led to a significant stimulus-dependent decrease in reporter gene transcription (p = 0.0006; Student's t-test, two-tailed; Fig. 3a and Supplementary Fig. 2a). For all enhancers tested, activity-regulated changes in H3K27ac were strongly correlated with changes in reporter gene expression ($R^2 = 0.73$). We confirmed these findings by placing selected enhancers from each group into two additional luciferase reporter constructs (containing either an SV40 or a minimal TATA-box promoter) to ensure that the activity-dependent transcriptional regulatory activity of these enhancers was not an artifact of the *Nptx2* reporter plasmid (Supplementary Fig. 2). We also tested whether sites with increasing H3K27ac but lacking CBP/H3K4me1-enrichment could function as activity-regulated enhancers in this assay. Enhancers with increasing H3K27ac but without CBP/H3K4me1, were significantly less active than those enriched for CBP/H3K4me1 (p=0.0003 Student's t-test, two-tailed) (Supplementary Fig. 3). In total, these data suggest that the dynamic chromatin signature of increasing H3K27ac at CBP/H3K4me1-enriched enhancers is a specific and predictive signature of functional neuronal activity-dependent enhancers.

Although CBP/H3K4me1-enriched enhancers with increasing H3K27ac could activate reporter gene transcription in membrane-depolarized neurons, it remained possible that these enhancers might not function as activity-dependent enhancers in their normal genomic context. To address this issue we investigated whether enhancers with increasing H3K27ac in response to neuronal activity are located near activity-regulated genes. For this analysis we focused our attention on the four categories of CBP/H3K4me1-enriched sites described above as well as the enhancers with increasing H3K27ac in the absence of detectable CBP and/or H3K4me1 enrichment. Regulatory regions from each of these groups of sites were assigned to the closest gene with detectable expression in neurons, and the expression of these genes was quantified using previously generated RNA-seq data[18]. Strikingly, we found that the expression level of genes closest to these enhancers was highly correlated with the level of H3K27ac both before and after membrane depolarization (Fig. 3b). Enhancers with increased H3K27ac in response to neuronal activity were associated with activity-dependent increases in the expression of the nearest gene ($p = 7.83 \times 10^{-11}$; paired Wilcoxon signed rank test), and the expression of genes associated with enhancers that had constant H3K27ac was higher before and after depolarization than the expression of genes associated with loci with no H3K27ac. Moreover, the expression of genes nearest these two classes of activity-independent enhancers exhibited a less dramatic increase in expression in response to neuronal activity than genes located near enhancers that display an activity-dependent increase in H3K27ac (Fig. 3b). Interestingly, in the aggregate the sites with increasing H3K27ac but without enrichment for CBP/H3K4me1 also exhibited a correlation with activity-dependent expression of the closest gene, suggesting that these sites also

function as enhancers in the context of chromatin (Fig. 3c), despite their apparent lack of function in luciferase reporter assays described above (Supplementary Fig. 3).

Taken together these experiments indicate that the subset of CBP/H3K4me1-enriched sites that function as activity-regulated enhancers can be identified by the presence of an increase in H3K27ac in response to neuronal activity. In addition, sites with increasing H3K27ac but lacking CBP/H3K4me1-enrichment are also likely to be activity-dependent enhancers (given their correlation with activity-dependent gene expression); however, they exhibit significantly lower levels of enhancer function when measured in luciferase reporter assays. Of the 11,830 previously identified activity-regulated enhancers (H3K4me1-enriched sites with activity-inducible CBP binding), 1468 display at least a two-fold increase in H3K27ac signal and robustly drive expression of a reporter gene in luciferase assays and can thus be categorized as bona fide activity-regulated enhancers in cultured neurons (Fig. 2c). These loci will henceforth be referred to as activity-regulated enhancers.

In vivo function of activity-regulated enhancers

To test if the activity-regulated enhancers identified in cultured cortical neurons function in the intact brain we determined if they overlap with DNaseI hypersensitive sites (DHS) identified in the developing brain and adult mouse cortex by the mouse ENCODE project[26,27]. Sensitivity of chromatin to digestion by DNaseI allows for the identification of genomic regions that are bound by transcription factors, and thus facilitates mapping of regulatory elements *in vivo*, including enhancers[28]. We found that ~99% of the activity-regulated enhancers identified in cultured neurons overlap with a DHS that has been mapped in published data sets in the mouse brain (E14.5 whole brain, E18.5 whole brain, adult cortex)[27]. This provides strong evidence that activity-regulated enhancers identified in cultured cortical neurons are also utilized during brain development and maturation. Interestingly, the degree of overlap between the activity-regulated enhancers and DHS sites was greater in the adult cortex (955/1468; 65.1%) than in E14.5 whole brain (515/1468; 35.1%) or E18.5 whole brain (644/1468; 43.9%). This suggests that many activity-regulated enhancers may not exhibit transcription factor binding until after birth, when sensory inputs increase the activity of cortical circuits and induce activity-regulated transcription in cortical neurons[3].

To further establish the *in vivo* relevance of the activity-regulated enhancers that we had identified in cultured cortical neurons, we asked if there was any overlap between our activity-regulated enhancers and those present in a recently published H3K27ac ChIP-seq dataset of active forebrain enhancers identified across embryonic and postnatal brain development (E11.5, E14.5, E17.5, p0, p7, p21 and p56)[29]. Towards this end, we generated an aggregated dataset of distal H3K27ac peaks from all of the stages of brain development (N = 42608 peaks, see methods) and determined the overlap between the *in vivo* forebrain enhancers and the activity-regulated enhancers identified in cultured cortical neurons. This analysis revealed that the majority (74% of + KCl enhancers) of the activity-regulated enhancers in membrane depolarized cortical neurons overlap with H3K27ac enhancers identified in the forebrain.

Given that the experiments to identify *in vivo* forebrain enhancers were performed using whole forebrain tissue from animals living in standard housing (no acute sensory stimulation), it is possible that H3K27ac ChIP-seq is not sufficiently sensitive to identify all of the neuronal activity-dependent enhancers that we detected in our *in vitro* cell culture experiments, as only a small fraction of cells in the intact cortex are engaged in activity-regulated transcription at any given time. However, taken together, these data indicate that the activity-dependent enhancers that we have identified in cultured cortical neurons also function in the intact cortex during embryonic and post-natal brain development.

Sequence determinants of activity-regulated enhancers

To assess how activity-regulated enhancers function to regulate gene transcription we performed *de novo* motif analysis to identify transcription factor binding motifs that are enriched in activity-regulated enhancers. The motif that was most significantly enriched among activity-regulated enhancers was the AP-1 motif (686 total AP-1 sites among 1468 peaks of the activity-regulated enhancers; MEME motif score $E=1.3e^{-194}$; Fig. 4a and Supplementary Fig. 4a)[30]. In parallel we also determined the correlation between defined sequence motifs and membrane depolarization-induced changes in H3K27ac levels using an independent method that did not rely on the thresholded H3K27ac classes, which represent only the subset of CBP/H3K4me1 enriched sites that have the most distinct H3K27ac dynamics (see methods). This analysis identified three motifs with the highest correlation with increasing H3K27ac at enhancers; the AP-1 motif (1.41 average fold change in H3K27ac ChIP-signal with depolarization, n=3962 enhancers), the CREB motif (1.75 fold change, n=175 enhancers), and the MEF2 motif (1.08 fold change, n=2946 enhancers). In addition, the E-box motif (0.87 fold change, n=5011 enhancers) was correlated with a significant decrease in H3K27ac signal in response to depolarization (Supplementary Table 1).

The transcription factor complex that binds preferentially to AP-1 sites consists of heterodimers of FOS and JUN family proteins, several of which (FOS, FOSB, JUNB) are robustly induced by neuronal activity[4]. While JUN family members, but not FOS family members, can homodimerize, FOS/JUN heterodimers form preferentially when FOS family members are present, as is the case when neurons are exposed to sensory stimuli[13]. Since the prevailing view was that in response to extracellular stimuli FOS/JUN complexes bind AP-1 sites within the promoters of late-response genes, we were surprised to find that the AP-1 motif is so frequently present in activity-regulated enhancers. It had not previously been considered that FOS/JUN family hetero-dimers might function primarily at enhancers in neurons.

FOS binding at neuronal activity-inducible enhancers

Given the enrichment of the AP-1 motif within activity-dependent enhancers we used ChIP-seq to determine if FOS binds to these enhancers. Cortical neurons were left unstimulated or exposed to elevated levels of KCl for two hours to achieve maximal induction of FOS protein. Under these conditions, we detected 12,594 FOS binding sites that were reproducibly detected across multiple experiments (Fig. 4b–c) and specific for the FOS protein based on ChIP-seq experiments with Fos shRNA (Supplementary Fig. 5a–b; see

methods). Among these 12,594 FOS peaks, 80.3% contained an AP-1 motif, further suggesting that these sites were bound by FOS. ChIP-seq using anti-JUNB and anti-FOSB antibodies revealed a significant enrichment for inducible binding of these additional AP-1 transcription factors at FOS binding sites suggesting that FOS/JUN heterodimers likely bind to activity-regulated enhancers (Fig. 4d). We note that only a fraction of activity-regulated enhancers defined in Fig. 2c (increasing H3K27ac group) are bound by FOS (621/1468, 42%), suggesting that FOS binding alone does not determine whether or not an enhancer functions in an activity-dependent manner (Fig. 4g–h).

Surprisingly, an analysis of the localization of FOS binding sites across the genome indicated that FOS is bound predominantly to gene-distal sites, with the overwhelming majority located greater than 1kb from an annotated transcriptional start site (96% of FOS binding sites; Fig. 4c). Furthermore, we find that in membrane depolarized neurons FOS binding sites are enriched for previously documented features of enhancers (H3K4me1, H3K27ac, CBP binding and PolII binding), suggesting that in cultured cortical neurons, activity-inducible AP-1 transcription factors bind predominantly to enhancers (Fig. 4e–g). In this respect FOS binding differs from that of most other transcription factors, which have a less marked bias towards enhancer binding[31]. This could suggest that in response to extracellular stimuli FOS functions in a specialized manner at enhancers to promote gene transcription.

Given that FOS peaks at activity-dependent enhancers represent a relatively small fraction of all FOS peaks, we next sought to determine whether all or a subset of distal genomic sites bound by FOS have activity-regulated enhancer function. To accomplish this, we selected FOS-bound, gene-distal sites with different levels of CBP binding and H3K27ac enrichment, cloned these elements into the *Nptx2* reporter construct, and tested their ability to function as activity-regulated enhancers. Consistent with our previous data (Fig. 3a), we found that only FOS binding sites that exhibit both CBP binding and increasing H3K27ac in response to neuronal activity drive activity-dependent reporter expression (Supplementary Fig. 3a). At the genome-wide level, FOS binding was detected at CBP/H3K4me1-enriched enhancers that displayed each of the changes in H3K27ac behavior described above, however, enhancers that displayed an increase in H3K27ac upon membrane depolarization exhibited the highest level of FOS binding (42% bound; Fig. 4h and Supplementary Fig. 6b–d). FOS binding was also observed at sites with increasing H3K27ac but no CBP/H3K4me1 enrichment (Supplementary Fig. 6e). In total, these data suggest that the functionally active FOS-bound enhancers in membrane depolarized neurons are the gene-distal FOS binding sites that are also bound by CBP/H3K4me1 and exhibit an increase in H3K27ac in response to membrane depolarization. It is likely that these FOS enhancers are also functionally active in the intact cortex given that 64.4% of the FOS enhancers that we identified in membrane depolarized cortical neurons are also enriched for H3K27ac in the forebrain *in vivo*.

Function of AP-1 binding at activity-regulated enhancers

Having shown that FOS binds to activity-regulated enhancers, we next tested whether FOS binding to these enhancers is required for enhancer activity. Towards this end, we tested

eight different activity-inducible enhancers that exhibited high levels of FOS binding for their ability to drive activity-dependent expression of the *Nptx2* promoter luciferase reporter gene. We then compared the level of induction by each enhancer with an identical enhancer in which each of the AP-1 sites was mutated by a single base pair to disrupt FOS binding (see methods). While all eight wild-type enhancers could confer activity-dependent luciferase expression when cloned into the reporter gene, mutation of the FOS binding sites led to significantly reduced reporter gene transcription in each case, often to a level exhibited by the reporter gene in the absence of the enhancer (Fig. 5a). This suggests that FOS binding is required for the activity-dependent function of each of these enhancers. In further support of this conclusion, we found that the ability of each of the activity-dependent, FOS bound enhancers to promote activity-dependent reporter gene expression was significantly diminished by co-transfection with an shRNA that targets *Fos*, compared to a control shRNA (Fig. 5b). Taken together, these findings suggest a model in which *Fos* expression is induced in response to neuronal activity, FOS together with a JUN family member (e.g. JUNB) binds to enhancer sequences throughout the genome, and the subset of these enhancers that exhibit CBP/H3K4me1-enrichment and increasing H3K27ac then function to promote activity-dependent gene expression. The fact that a subtle mutation in the FOS binding site in an enhancer can have a dramatic effect on reporter gene transcription suggests that when similar mutations occur in endogenous activity-regulated enhancers they may have significant effects on sensory stimulus-dependent gene transcription.

Identification of FOS target genes in neurons

The finding that FOS controls enhancer activity across the neuronal genome suggests that FOS likely regulates a large number of activity-dependent genes that are important for nervous system development and function. However, while the induction of *Fos* in the brain has been extensively studied for several decades to date there has been no attempt to identify the targets of FOS at a genome-wide level, and it was not known how many genes FOS activates in a given cell. To identify potential FOS target genes, we performed microarray analysis on RNA obtained from mouse cortical neurons infected with lentivirus containing either a control shRNA or *Fos* shRNA that were subsequently depolarized for 0, 1, 3, or 6 hours with KCl treatment. We then assessed the effect of reducing FOS protein levels on the expression of individual activity-regulated genes. Western blot analysis of protein lysates obtained from paired cortical cultures demonstrated that *Fos* shRNA nearly completely blocked induction of FOS protein at each timepoint of KCl stimulation examined (Fig. 6a). Importantly the induction of FOSB or the levels of several activity-dependent post-translational modifications (MEF2D de-phosphorylation, MECP2 phosphorylation at serine 421, CREB phosphorylation at serine 133) were unchanged, indicating that activity-regulated signaling overall was not affected by lentiviral infection and *Fos* shRNA expression (Fig. 6a).

To determine the effect of *Fos* knockdown on activity-regulated gene transcription, we focused our analysis on activity-regulated genes (genes in control shRNA infected cultures that were upregulated at least 3-fold in response to KCl compared to the unstimulated condition; Figure 6B, red) and compared their induction between the control shRNA and *Fos* shRNA conditions. *Fos* shRNA reduced induction of 187/376 activity-regulated genes

by at least 1.5 fold, suggesting that FOS is important for the proper transcriptional activation of a substantial fraction of the activity-regulated gene program in cortical neurons (Supplementary Table 2). To determine which of these putative FOS target genes are directly regulated by FOS, we determined which activity-regulated genes that are down-regulated by *Fos* shRNA also have a FOS ChIP-seq peak located nearby (within 100 kb of the transcription start site) that exhibits activity-regulated enhancer features (CBP/H3K4me1-enrichment, increasing H3K27ac in response to neuronal activity). For this purpose, we considered all CBP/H3K4me1-enriched enhancers that have an increase in H3K27ac, rather than including only enhancers that exhibit the largest fold increases (i.e. the previously defined "increasing H3K27ac" group). Of the 187 putative FOS target genes, 53 met these criteria (Supplementary Table 2). These data suggest that a significant fraction of the genes misregulated by FOS knockdown are likely to be direct FOS targets. However, it is important to note that loss of FOS function can be partly compensated for by FOSB, as well as more distantly related AP-1 family members such as FOSL1 and FOSL2[32]. Therefore, it is possible that the identification of direct targets of FOS using the criteria described above might underestimate the number of enhancers that require AP-1 heterodimer binding for their function. This is consistent with the results of the AP-1 loss-of-function luciferase reporter assays (Fig 5a–b) demonstrating more dramatic effects on reporter expression when the AP-1 motif was mutated compared to co-transfection with *Fos* shRNA.

Among direct FOS targets were genes known to be important for activity-regulated processes in neurons including the postsynaptic scaffolding protein GRASP that has been shown to regulate metabotropic glutamate receptors[33], the secreted protein NPTX2 that regulates AMPA receptor clustering, homeostatic scaling and critical-period plasticity[7,34,35], the hormone IGF1 that has been shown to be important for brain development[36], and the histone deacetylase HDAC9 that is highly expressed within the nervous system and is thought to regulate dendrite development (Fig. 7b)[37]. Importantly, the majority of these direct FOS target genes (10/14) were effectively induced in the cortex upon exposure of dark reared mice to light (Fig. 8). This indicates that these FOS targets also mediate the effects of sensory stimuli in the intact brain.

Taken together, these findings suggest that sensory stimuli that induce *Fos* in the brain trigger FOS binding to thousands of enhancer sequences across the genome, and that via a subset of these enhancers (e.g. the enhancers that are enriched for CBP/H3K4me1 and exhibit increasing H3K27ac in response to neuronal activity), FOS induces changes in gene expression that underlie the neuronal response to sensory stimuli.

DISCUSSION

In this study, we identify a dynamic chromatin signature that enables the comprehensive mapping of the enhancers that promote activity-regulated transcription in cortical neurons. Although previous work had identified ~12,000 putative neuronal activity-regulated enhancers based on CBP/H3K4me1-enrichment, we demonstrate that only the subset of these sites that is rapidly acetylated at H3K27 in response to neuronal activity can drive activity-regulated transcription. Having identified these functional *cis*-regulatory sites, we

demonstrate that a common feature of many of these enhancers is their ability to bind the activity-induced transcription factor FOS. The induction of *Fos* in response to membrane depolarization is critical for activity-dependent enhancer function and for activation of a large subset of the genes that comprise the neuronal activity-regulated gene program. These findings suggest a pervasive and previously unappreciated function for FOS at neuronal activity-regulated enhancers.

In recent years, the ability to comprehensively identify the enhancers that are active in a given cellular state has provided important insight into the transcriptional regulatory events that govern cell fate specification during development. However, it was not known whether stimulus-responsive enhancers would exhibit the same features as constitutively active enhancers. Thus, identification of a chromatin signature that specifically marks the subset of cellular enhancers that control neuronal activity-dependent gene expression (increased H3K27ac in response to membrane depolarization), represents an important step towards characterizing the mechanism of action and the biological functions of stimulus-responsive enhancers.

Despite its widespread use in enhancer identification, the function of H3K27ac, and its regulation by histone acetyltransferases and histone deacetylases, are not well characterized[24]. H3K27ac is thought to be catalyzed by CBP, a histone acetyltransferase and transcriptional co-activator that binds to as many as 12,000 enhancers when neurons are exposed to a depolarizing stimulus[18]. However, our data indicate that only a small fraction (12.4%; 1468/11830) of these CBP-bound enhancers exhibit activity-induced increases in H3K27ac, suggesting that recruitment of CBP to an enhancer in response to neuronal activity is not sufficient to initiate H3K27 acetylation. Taken together with several recent studies in other cell types, our findings suggest that there are likely to be additional factors that regulate the acetyltransferase activity of CBP (and the highly related histone acetyltransferase p300) once it is bound to enhancers[22,23]. Furthermore, we provide evidence that sites with increasing H3K27ac but without detectable CBP/H3K4me1 enrichment function as enhancers in the context of native chromatin (but not in luciferase reporter assays). It will be important to determine whether this is the result of differences in sensitivity of detection of CBP binding compared to H3K27ac. If the sensitivity of CBP detection by ChIP-seq is low, it could be difficult to detect CBP binding at enhancers with observable changes in H3K27ac that are bound by CBP only in a specific subset of neurons present in the mixed cortical cultures. As ChIP-seq techniques mature, it should be possible to investigate enhancer function in specific neuronal cell types, which will be required to further investigate these issues. In neurons, CBP binding is largely activity-regulated, as relatively few CBP binding sites (~1000) were detected prior to membrane depolarization. Given the importance of CBP for Rubinstein-Taybi syndrome, as well as increasing evidence that HDACs are critical mediators of activity-regulated transcription and are mutated in human disorders of cognitive function, it will be important to characterize the specific functions of these histone-modifying complexes at activity-regulated enhancers in neurons[38].

The comprehensive identification of the enhancers that promote activity-dependent gene transcription in cultured cortical neurons is a first step in understanding how this class of

enhancers functions to initiate and/or amplify gene transcription in the brain during learning, memory, and behavior. It is likely that the activity-dependent enhancers that we have identified in cultured neurons function in a similar manner in the brain in response to sensory stimuli given that these regulatory elements are DNaseI hypersensitive and enriched for H3K27ac in the brain, and the genes these enhancers regulate are induced in the cortex of dark reared mice that have been exposed to light. However, the importance of FOS at activity-dependent enhancers *in vivo* remains to be established. Our efforts to detect FOS binding by ChIP-qPCR at activity-regulated enhancers in brain extracts from mice that were dark reared and exposed to light have so far been unsuccessful. This may reflect the increased heterogeneity of neurons in the intact cortex, and possibly the fact that activity-dependent enhancers function in a cell type-specific manner resulting in a much larger repertoire of FOS-bound enhancers *in* vivo that are difficult to detect in a heterogeneous population of neurons.

Although early-response transcription factors such as FOS are thought to be critical for stimulus-responsive transcription in virtually all cell types in the body, our understanding of how these transcription factors activate transcription of their target genes in a cell type-specific manner is incomplete. In the nervous system, transcription of early-response genes encoding transcription factors including *Fos*, *Fosb*, *Junb*, *Nr4a1*, *Egr1* and *Npas4* has been used to mark neurons that are activated by sensory input, and the induction of these transcription factors is thought to be required for the proper activation of late-response genes, which include critical regulators of dendrite development, synaptic maturation and circuit plasticity. By mapping the binding sites of the AP-1 transcription factors FOS, FOSB and JUNB in membrane depolarized cortical neurons, we discovered that the vast majority of binding sites for these factors are located far away from the start sites for gene transcription. The extreme preference of AP-1 transcription factors for binding to enhancers suggests that FOS/JUN heterodimers may function in a unique manner at enhancers that is specifically tailored to enhancer function and different from the mechanism by which transcription factors function at promoters. Further studies of FOS may provide new insight into how transcription factors bound to enhancers are capable of promoting transcription by acting from a location that is far from the site of transcriptional initiation. .

The identification of the FOS-bound enhancers in cortical neurons has allowed us to identify over 50 direct FOS target genes in these cells. These FOS target genes include well-characterized regulators of synaptic development and plasticity such as *Nptx2*, *Igf1*, *Grasp*, and *Hdac9* indicating that even though *Fos* can be induced in essentially all mammalian cell types, in neurons FOS activates targets that have neuronal specific functions. It will be interesting to determine how these FOS targets are specified during neural development. Given the diversity of cell types in the nervous system it seems likely that the functional activity-regulated enhancers as well as FOS-bound enhancers will also be found to differ from one neuronal cell type to another. It will be useful in the future to define the range of FOS-bound, activity-regulated enhancers in different types of neurons as this has the potential to reveal in greater depth how sensory inputs through FOS specify neuronal responses in the developing and mature nervous system.

EXPERIMENTAL PROCEDURES

Mouse cortical neuron culture

Embryonic day 16.5 (E16.5) C57BL/6 embryonic mouse cortices were dissected and then dissociated for 10 minutes in 1× Hank's Balanced Salt Solution (HBSS) containing 20 mg/mL trypsin (Worthington Biochemicals) and 0.32 mg/mL L-cysteine (Sigma). Trypsin treatment was terminated by washing dissociated cells three times for two minutes each in dissociation medium consisting of 1× HBSS containing 10 mg/mL trypsin inhibitor (Sigma). Cells were then triturated using a flame-narrowed Pasteur pipette to fully dissociate cells. After dissociation, neurons in were kept on ice in dissociation medium until plating. Cell culture plates were pre-coated overnight with a solution containing 20 μg/mL poly-D-lysine (Sigma) and 4 μg/mL mouse laminin (Invitrogen) in water. Prior to plating neurons, cell culture plates were washed three times with sterile distilled water and washed once with Neurobasal Medium (Life Technologies). Neurons were grown in neuronal medium consisting of Neurobasal Medium containing B27 supplement (2%; Invitrogen), penicillin-streptomycin (50 g/ml penicillin, 50 U/mL streptomycin, Sigma) and glutamine (1 mM, Sigma). At the time of plating, cold neuronal medium was added to neurons in dissociation medium to dilute neurons to the desired concentration. Neurons were subsequently plated and placed in a cell culture incubator that maintained a temperature of 37° C and a CO_2 concentration of 5%. Two hours after plating neurons, medium was completely aspirated from cells and replaced with fresh warm neuronal medium. Neurons were grown *in vitro* until the seventh day *in vitro* (DIV7). For ChIP-Seq experiments, mouse cortical neurons were plated at an approximate density of 4×10^7 on 15-cm dishes. Neurons were plated in 30mL neuronal medium. Ten mL of the medium was replaced with 12 ml fresh warm medium on DIV3 and DIV6.

For luciferase reporter assays, mouse cortical neurons were plated at an approximate density of 3×10^5 per well on 24-well plates. Neurons were plated in 500 μL neuronal medium. On DIV3, 100 μL fresh warm medium was added to neurons. On DIV5 neurons were transfected (see section on transfection). At the completion of transfection, conditioned medium containing 15% fresh medium was returned to neurons.

Stimulation with potassium chloride (KCl)

Prior to KCl depolarization, neurons were silenced with 1μM tetrodotoxin (TTX, Fisher) and 100μM DL-2-amino-5-phosphopentanoic acid (DL-AP5, Fisher). Neurons were subsequently stimulated by adding warmed KCl depolarization buffer (170 mM KCl, 2 mM CaCl2, 1 mM MgCl2, 10 mM HEPES) directly to the neuronal culture, to final concentration of 31% in the neuronal culture medium within the culture plate or well. For KCl depolarization of neurons for ChIP-Seq experiments, DIV 6 neurons were silenced overnight with 1μM TTX and 100μM DL-AP5. The next morning, neurons were left silenced (–KCl condition) or stimulated for 2 hours with KCl (+KCl condition). For KCl depolarization of neurons for luciferase reporter assays, DIV 7 neurons were silenced for two hours with 1μM TTX and 100μM DL-AP5. Two hours later, neurons were left silenced (–KCl condition) or stimulated for 6 hours with KCl (+KCl condition).

ChIP-Seq

40 million mouse cortical neurons cultured to *in vitro* day 7 were used for each ChIP-seq library construction. Typically 20–40 million cortical neurons were used for a single ChIP experiment. To cross-link protein-DNA complexes, media was removed from neuronal cultures and crosslinking-buffer (0.1 M NaCl, 1 mM EDTA, 0.5 mM EGTA, 25 mM HEPES-KOH, pH 8.0) containing 1% formaldehyde was added for 10 minutes at room temperature (RT). Cross-linking was quenched by adding 125 mM glycine for five minutes at RT. Cells were then rinsed three times in ice-cold PBS containing complete protease inhibitor cocktail tablets (Roche) and collected by scraping. Cells were pelleted and either stored at −80° C until use or immediately processed. Cell pellets were lysed by 20 cell pellet volumes (CPVs) of buffer 1 (50 mM HEPES-KOH, pH 7.5, 140 mM NaCl, 1 mM EDTA, pH 8.0, 10 % Glycerol, 0.5 % NP-40, 0.25 % Triton X-100, complete protease inhibitor cocktail) for 10 min at 4° C. Nuclei were then pelleted by centrifugation at 3000 rpm for 10 min at 4° C. The isolated nuclei were rinsed with 20 CPVs of buffer 2 (200 mM NaCl, 1 mM EDTA, pH 8.0, 0.5 mM EGTA, pH 8.0, 10 mM Tris-HCl, pH 8.0, complete protease inhibitor cocktail) for 10 min at RT and re-pelleted. Next, 4 CPVs of buffer 3 (1 mM EDTA, pH 8.0, 0.5 mM EGTA, pH 8.0, 10 mM Tris-HCl, pH 8.0, complete protease inhibitor cocktail) were added to the nuclei and sonication was carried out using a Misonix 3000 Sonicator (Misonix) set at a power setting of 7.5 (equivalent to 24 watts). 20 pulses of 15 s each were delivered at this setting, which resulted in genomic DNA fragments with sizes ranging from 200 bp to 2 kb. Insoluble materials were removed by centrifugation at 20,000 rpm for 10 min at 4° C. The supernatant was transferred to a new tube and the final volume of the resulting nuclear lysate was adjusted to 1 mL by adding buffer 3 supplemented with 0.3 M NaCl, 1 % Triton X-100, 0.1 % deoxycholate. The lysate was pre-cleared by adding 100 μL of pre-rinsed Protein A/G Agarose (Sigma) per 1 ml of the lysate and incubating for 1 hour at 4 ° C. After pre-clearing, ten percent of the ChIP sample (50 uL from 500 μL lysate) was saved as input material. The remaining lysate was incubated with antibodies for immunoprecipitation. The antibody incubation was carried out overnight at 4 ° C. The next day, 30 uL of pre-rinsed Protein A/G PLUS Agarose beads (Santa Cruz Biotechnology) was added to each ChIP reaction and further incubated for 1 hour at 4 ° C. The beads bound by immune-complexes were pelleted and washed twice with each of the following buffers: low salt buffer (0.1% SDS, 1% Triton X-100, 2 mM EDTA, 20 mM Tris-HCl, pH 8.1, 150mM NaCl), high salt buffer (0.1% SDS, 1% Triton X-100, 2 mM EDTA, 20 mM Tris-HCl, pH 8.1, 500 mM NaCl) and LiCl buffer (0.25 M LiCl, 1% IGEPAL CA630, 1% deoxycholic acid (sodium salt), 1 mM EDTA, 10 mM Tris, pH 8.1). In each wash, the beads were incubated with wash buffer for 10 min at 4° C while nutating. The washed beads were then rinsed once with 1x TE buffer (10 mM Tris-HCl, pH 8.0, 1 mM EDTA). The immunoprecipitated material was eluted from the beads twice by adding 100 μL of elution buffer (10 mM Tris-HCl, pH 8.0, 1 mM EDTA, pH 8.0, 1 % SDS) to each ChIP reaction and incubating the sample at 65° C for 30 min with brief vortexing every 2 min. 150 μL of elution buffer was also added to the saved input material (50 μL) and this sample was processed together with the ChIP samples. The eluates were combined and crosslinking was reversed by incubation at 65° C overnight. The next day, 7 μg RNase A (affinity purified, 1mg/mL; Invitrogen) was added to each sample and samples were incubated at 37° C for one hour. Then, 7 μL Proteinase K (RNA grade, 20 mg/mL; Invitrogen) was added to each

sample and samples were incubated at 55° C for two hours. The immunoprecipitated genomic DNA fragments were then extracted once with Phenol:Chloroform:Isoamyl Alcohol (25:24:1, pH 7.9; Life Technologies) and then back extracted with water. The resulting genomic DNA fragments were then purified using the QIAquick PCR purification kit (Qiagen) and DNA fragments were eluted in 100 μl of Buffer EB (elution buffer consisting of 10 mM Tris-HCl, pH 8.5, Qiagen). Samples were assessed for enrichment by quantitative PCR using primers to different genomic regions. Samples with significant enrichment over negative regions were submitted to the Beijing Genomic Institute (BGI) for 50 base pair single end sequencing on the Illumina Hiseq 2000 platform. For each sample, over 20 million clean reads were obtained.

Antibodies

The following antibodies were used: H3K27ac (Abcam, ab4729), FOS (Santa Cruz, sc-52; primary antibody used for ChIP-seq) FOS (Santa Cruz, sc-7202; used for an additional ChIP-seq replicate and for western blotting for FOS, Fig. 4b, Fig. 6a and Supplementary Fig. 5a), FOSB (Santa Cruz, sc-48), JUNB (Santa Cruz, sc-46), phospho-CREB (Ser133) (Millipore, clone 10E9), MEF2D (BD biosciences; Cat. No. 610774), MECP2-p421 (generated in the Greenberg lab[39])

ChIP-Seq Analysis

Sequencing data was obtained from BGI in gzipped fastq file format. Files were transferred and unzipped. Then, sequencing reads were aligned to the July 2007 assembly of the mouse genome (NCBI 37, mm9) using the Burrows-Wheeler Aligner (BWA) with default settings[40]. The resulting bwa files were then converted to sam files and uniquely mapped reads were extracted from the sam files. Sam files of the uniquely mapped reads were then converted to bam files. Bam files were then used for peak calling using Model-based Analysis of ChIP-Seq (MACS)[41] with the following parameters: -f BAM -g mm --nomodel --shiftsize=150. To visualize ChIP-Seq data on the UCSC genome browser, ChIP-Seq bam files were converted to bigwig track format to display the number of input normalized ChIP-Seq reads, normalized to 20 million total reads.

H3K27ac peaks were classified based on their location relative to genes in the NCBI Reference Sequence Database (RefSeq). H3K27ac peaks were classified as being proximal if they were within 1kb of an annotated transcriptional start site (TSS). H3K27ac peaks were classified as being distal if they were greater than 1kb from an annotated transcriptional start site (TSS). Distal H3K27ac peaks were further classified as intragenic if they occurred within a RefSeq gene, or as extragenic if they did not occurred within a RefSeq gene. For chromatin modifications (H3K4me1, H3K27ac), the number of input-normalized ChIP-Seq reads within a 2 kb window centered on each enhancer was taken to be the ChIP-Seq signal at the enhancer. For transcription factors (CBP), the number of input-normalized ChIP-Seq reads within an 800 bp window centered on each enhancer was taken to be the ChIP-Seq signal at the enhancer.

Enhancers were classified into different categories based on the behavior of the quantified H3K27ac signal at each enhancer. Enhancers were classified as having increasing H3K27ac

if they exhibited a two fold or greater increase in H3K27ac signal with stimulation and if the stimulated signal for H3K27ac was not within the bottom quartile of H3K27ac signal at all enhancers identified in the stimulated condition. Enhancers were classified as having decreasing H3K27ac if they exhibited a two fold or greater decrease in H3K27ac signal with stimulation and if the unstimulated signal for H3K27ac was not within the bottom quartile of H3K27ac signal at all enhancers identified in the unstimulated condition. Enhancers were classified as having constant H3K27ac if they exhibited H3K27ac signal in the top quartile of all enhancers identified in both the unstimulated and stimulated conditions and if the H3K27ac signal changed by 10% or less with stimulation. Enhancers were classified as having no H3K27ac if they were identified previously on the basis of inducible CBP binding and enrichment for H3K4me1[18] but did not overlap with H3K27ac peaks within the H3K27ac datasets generated in this study.

For FOS ChIP-seq, three biological replicates were performed from paired membrane depolarized and unstimulated neuronal cultures using an anti-FOS antibody (sc-52; Santa Cruz Biotechnology), and two of these three replicates included in additional paired sample of neurons infected with FOS shRNA lentivirus in pLL3.7 (to confirm the specificity of this antibody). MACS identified 19,077 peaks called over input chromatin (using default threshold parameters: MACS p= 1×10^{-5}) that were reproducibly detected in 2/3 biological replicates. Of these sites, the ChIP-seq signal at 12,594 was reduced by least 50% in 2/2 shRNA experiments. We focused our further analysis on this set of reproducible and specific FOS peaks for subsequent analysis. In addition, we performed one further replicate of FOS ChIP-seq with a second anti-FOS antibody (sc-7202; Santa Cruz Biotechnology) to further confirm the specificity of these peaks (Fig. 3b, Supplementary Fig. 3a).

RNA-Seq analysis

RNA-Seq data from a previous study[18] were analyzed and integrated into this study. For nearest gene analyses, the nearest gene (with non-zero expression) to an enhancer was linked to that enhancer and the expression of the genes nearest to each class of enhancers was characterized.

Neuronal Transfection

Mouse cortical neurons plated on 24 well plates at a density of approximately 3×10^5 neurons per well were transfected for luciferase reporter assays using Lipofectamine 2000 Reagent (Invitrogen), according to the manufacturer's protocol with slight modifications. Briefly, DNA mixes were made immediately preceding the transfection consisting of 1 μg total plasmid DNA/well diluted in Neurobasal medium (Life Technologies). DNA typically consisted of 450 ng firefly luciferase reporter DNA, 50ng pGL4.74 renilla luciferase reporter DNA (Promega), and 500 ng empty pCS2 plasmid[42] as filler DNA. Lipofectamine was used at 2 μL/well and was diluted in Neurobasal medium just before the transfection. Within each experiment, all conditions were transfected in two to three independent wells, for technical duplicates or triplicates. Thirty minutes prior to the addition of Lipofectamine to neurons, the culture medium was removed and replaced with warmed Neurobasal medium. At this time, neurons were returned to the incubator and DNA mixes were added to diluted Lipofectamine in a drop-wise manner. After thirty minutes of incubation, DNA-

Lipofectamine mixes were added to neurons, again in a drop-wise manner. The cells were left to incubate with the DNA-Lipofectamine mix for two hours, after which the transfection medium was replaced with supplemented conditioned neuronal medium.

After stimulation, neurons were lysed using Passive Lysis Buffer (Dual-Luciferase Reporter Assay System, Promega). Lysates were then collected in microcentrifuge tubes and frozen at −20° C. At the time of performing the luciferase assay, neuronal lysates were thawed, briefly vortexed, briefly spun down, and then 20 μL of each sample was added to one well of Costar White Polystyrene 96-well Assay Plates (Corning). The reagents to run the luciferase assay, Luciferase Assay Reagent II (LARII) and Stop & Glo Reagent (Dual-Luciferase Reporter Assay System, Promega), were aliquoted and thawed according to the manufacturer's protocol. The luciferase assay was performed using the Synergy 4 Hybrid Microplate Reader (BioTek), with 100 μL of LARII and Stop & Glo Reagent injected per well. Data was subsequently downloaded and analyzed using Microsoft Excel.

Using the Dual-Luciferase Reporter Assay System, we recorded Firefly (FF) and Renilla (Ren) luminescence from each well. To correct for variations in transfection efficiency and cell lysate generation, the Firefly values were normalized to Renilla luminescence within each well, generating a ratio of FF/Ren. The stimulus-dependent fold induction of each reporter plasmid was obtained by dividing the (+ stimulus) FF/Ren value by the (– stimulus) FF/Ren value. To isolate the induction due to the enhancer, the fold induction of an enhancer reporter was divided by the fold induction of the appropriate backbone into which the enhancer was cloned, giving fold induction relative to backbone. Fold induction relative to backbone is the value shown in all figures containing luciferase reporter data.

Luciferase reporter assays

Most luciferase reporter plasmids used were based on the *Nptx2* gene, and hence this reporter was termed the *Nptx2* reporter. To develop the *Nptx2* reporter, we cloned the 4355 bp region upstream of the *Nptx2* coding sequence from C57BL/6 purified mouse genomic DNA between the NheI and EcoRV restriction sites within the multiple cloning site of the promoter-less pGL4.11 reporter plasmid (Promega) using sequence specific-primers primers (forward primer: GCGCGCTAGCTTCCTGGCTTGTAGTGACCT, reverse primer: GCGCGATATCCTCGCTGACCTGTGTGCTCACTTCA). pGL4.11 was chosen as the host plasmid since it contained the luc2P reporter gene, which contains an hPEST protein destabilization sequence. We found that the luc2P reporter responded more quickly and with greater magnitude to stimuli than luc2 reporters. Using PCR driven overlap extension the *Nptx2* reporter was then modified so that the 1216 bp *Nptx2* upstream enhancer (located −3607 to −2391 relative to the start of the *Nptx2* coding sequence) was replaced with a multiple cloning site containing SbfI, PacI, PmeI, and AscI restrictions sites[43]. The multiple cloning site was inserted into the *Nptx2* upstream regulatory region to create a modified Nptx2 reporter so that various enhancers could be easily cloned into this multiple cloning site. We verified that the modified *Nptx2* reporter in which the *Nptx2* enhancer had been cloned into the multiple cloning site had the same induction as the wild-type *Nptx2* reporter (data not shown). This suggested that the multiple cloning site did not affect the function of the reporter and that other enhancers could be similarly cloned into this multiple cloning site

without adverse affects on enhancer function. The pGL4.11 Nued2 reporter construct is available via Addgene (plasmid #59744).

To test enhancer function in additional reporter contexts, we generated two additional reporter constructs by modifying pGL4.24 (Promega), a luciferase reporter containing a minimal TATA box containing promoter but not containing any enhancer elements. To facilitate cloning of enhancers from the *Nptx2* reporter plasmid into this plasmid, we first modified this plasmid by adding a multiple cloning site containing SbfI, PacI, PmeI, and AscI sites between BamHI and SalI sites downstream of the firefly luciferase gene (pGL4.24_minP_MCS). We then further modified pGL4.24_minP_MCS by removing the minimal TATA box containing promoter from this plasmid and replacing this promoter with an SV40 promoter from another Promega luciferase reporter, the pGL3-Promoter Vector. This cloning was achieved by using BglII and NcoI restriction sites flanking both promoter regions. This resulted in the generation of a separate reporter construct, pGL4.24_SV40_MCS, with which enhancer activity could be assessed.

Enhancers with different H3K27ac behaviors were cloned between the SbfI and AscI sites within the multiple cloning site of the modified *Nptx2* reporter. Cloned enhancer regions varied in size but were approximately 1kb in length. Enhancers cloned using this strategy and the primers used to amplify each enhancer from mouse genomic DNA are listed in Supplementary table 3. For *Nptx2* reporter assays with FOS shRNA co-transfection, a scrambled version of an shRNA targeting *Npas4* in the pLL3.7 vector was used as the control[9].

Lentiviral infection of shRNA constructs

shRNAs targeting *Fos* (target sequence 5'GCCTTTCCTACTACCATTC'3) or a control hairpin targeting firefly luciferase (target sequence: CTTACGCTGAGTACTTCGA) were cloned into the pLL3.7 plasmid (Addgene Plasmid #11795). For lentiviral infections, neurons were cultured as described above. On DIV5, lentiviral supernatant was applied to cultures for 6h with 6 μg/mL polybrene. At DIV7, neurons were silenced and stimulated with KCl as described for either 0,1,3 or 6h and total RNA was purified using Trizol and the RNeasy mini kit from Qiagen. 10 μg of labeled cDNA was hybridized to Affymetrix mouse genome 430 2.0 arrays with affymetrix processing. Microarray experiments were performed at the Dana Farber Microarray Core facility.

qRT-PCR of FOS direct target genes from visual cortex

All experiments with mice were approved by the Animal Care and Use Committee of Harvard Medical School. For dark rearing, p49 animals (2 males and 2 females/condition) were placed into a dark chamber. At p56, animals were exposed to light for the indicated time periods. At the end of the light stimulus, visual cortices from each animal were removed and snap-frozen in liquid nitrogen. For RNA extraction, the visual cortex from each animal was solubilized in 1mL Trizol and RNA was extracted using Qiagen RNeasy mini kit according to the manufacturer's protocol. Complementary DNA was synthesized from 1 μg of input RNA using the ABI High Capacity cDNA synthesis kit with (random primed). 5 ng of cDNA/reaction was used for qPCR reactions. Reactions were run in

duplicate wells on a 384-well thermal cycler (Roche). Primers are listed in Supplementary Table 3.

Correlation of defined motifs with H3K27ac dynamics

H3K27ac peaks were called based on windows of at least 1000 bp in size that contained an average of >4 genome-normalized reads per base pair in the averaged pre and post stimulation data. Peaks that were within 2000 bp of transcriptional start sites were considered promoters, while the remainder were classified as distal enhancer-like elements. The top motifs underlying both of these regions were identified using Homer[44]. Homer was also used to identify the fraction of FOS ChIP-seq peaks that contain an AP-1 motif.

Analysis of *in vivo* H3K27ac data

Data from[29] was downloaded from GEO (GSE52386) and mapped to mm9 using bowtie allowing up to two mismatches and only retaining uniquely mapping reads. Reads mapping to identical locations were removed. Each dataset was normalized to the total number of uniquely mapping reads.

Supplementary Material

Refer to Web version on PubMed Central for supplementary material.

Acknowledgements

The authors would like to thank all of the members of the Greenberg lab for their scientific support and helpful discussions. This work was funded by the U.S. National Institutes of Health (NIH Project # 5R37NS028829-25 to M.E.G.), the National Institute of General Medical Sciences award number T32GM007753 (A.N.M.) and a National Cancer Institute Institutional Training Grant T32CA009361 (T.V.). T.V. and H.S. are both HHMI Fellows of the Damon Runyon Cancer Research Foundation. E.L. is supported by the National Science Foundation Graduate Research Fellowship under Grant Nos. DGE0946799 and DGE1144152. The content of this study is solely the responsibility of the authors and does not necessarily represent the official views of the funding sources mentioned.

References

1. Greer PL, Greenberg ME. From synapse to nucleus: calcium-dependent gene transcription in the control of synapse development and function. Neuron. 2008; 59:846–860. [PubMed: 18817726]
2. Leslie JH, Nedivi E. Activity-regulated genes as mediators of neural circuit plasticity. Progress in neurobiology. 2011; 94:223–237. [PubMed: 21601615]
3. Hensch TK. Critical period plasticity in local cortical circuits. Nature reviews. Neuroscience. 2005; 6:877–888.
4. Alberini CM. Transcription factors in long-term memory and synaptic plasticity. Physiological reviews. 2009; 89:121–145. [PubMed: 19126756]
5. Day JJ, Sweatt JD. Epigenetic mechanisms in cognition. Neuron. 2011; 70:813–829. [PubMed: 21658577]
6. Lyons MR, West AE. Mechanisms of specificity in neuronal activity-regulated gene transcription. Progress in neurobiology. 2011; 94:259–295. [PubMed: 21620929]
7. O'Brien RJ, et al. Synaptic clustering of AMPA receptors by the extracellular immediate-early gene product Narp. Neuron. 1999; 23:309–323. [PubMed: 10399937]
8. Hong EJ, McCord AE, Greenberg ME. A biological function for the neuronal activity-dependent component of Bdnf transcription in the development of cortical inhibition. Neuron. 2008; 60:610–624. [PubMed: 19038219]

9. Lin Y, et al. Activity-dependent regulation of inhibitory synapse development by Npas4. Nature. 2008; 455:1198–1204. [PubMed: 18815592]
10. Ebert DH, Greenberg ME. Activity-dependent neuronal signalling and autism spectrum disorder. Nature. 2013; 493:327–337. [PubMed: 23325215]
11. Greenberg ME, Ziff EB. Stimulation of 3T3 cells induces transcription of the c-fos proto-oncogene. Nature. 1984; 311:433–438. [PubMed: 6090941]
12. Greenberg ME, Ziff EB, Greene LA. Stimulation of neuronal acetylcholine receptors induces rapid gene transcription. Science. 1986; 234:80–83. [PubMed: 3749894]
13. Eferl R, Wagner EF. AP-1: a double-edged sword in tumorigenesis. Nature reviews. Cancer. 2003; 3:859–868.
14. Banerji J, Rusconi S, Schaffner W. Expression of a beta-globin gene is enhanced by remote SV40 DNA sequences. Cell. 1981; 27:299–308. [PubMed: 6277502]
15. Levine M. Transcriptional enhancers in animal development and evolution. Current biology : CB. 2010; 20:R754–R763. [PubMed: 20833320]
16. Heintzman ND, et al. Distinct and predictive chromatin signatures of transcriptional promoters and enhancers in the human genome. Nature genetics. 2007; 39:311–318. [PubMed: 17277777]
17. Visel A, et al. ChIP-seq accurately predicts tissue-specific activity of enhancers. Nature. 2009; 457:854–858. [PubMed: 19212405]
18. Kim TK, et al. Widespread transcription at neuronal activity-regulated enhancers. Nature. 2010; 465:182–187. [PubMed: 20393465]
19. Maurano MT, et al. Systematic localization of common disease-associated variation in regulatory DNA. Science. 2012; 337:1190–1195. [PubMed: 22955828]
20. Visel A, et al. A high-resolution enhancer atlas of the developing telencephalon. Cell. 2013; 152:895–908. [PubMed: 23375746]
21. Telese F, Gamliel A, Skowronska-Krawczyk D, Garcia-Bassets I, Rosenfeld MG. “Seq-ing” insights into the epigenetics of neuronal gene regulation. Neuron. 2013; 77:606–623. [PubMed: 23439116]
22. Creyghton MP, et al. Histone H3K27ac separates active from poised enhancers and predicts developmental state. Proceedings of the National Academy of Sciences of the United States of America. 2010; 107:21931–21936. [PubMed: 21106759]
23. Rada-Iglesias A, et al. A unique chromatin signature uncovers early developmental enhancers in humans. Nature. 2011; 470:279–283. [PubMed: 21160473]
24. Calo E, Wysocka J. Modification of enhancer chromatin: what, how, and why? Molecular cell. 2013; 49:825–837. [PubMed: 23473601]
25. Hsu YC, Perin MS. Human neuronal pentraxin II (NPTX2): conservation, genomic structure, and chromosomal localization. Genomics. 1995; 28:220–227. [PubMed: 8530029]
26. Shen Y, et al. A map of the cis-regulatory sequences in the mouse genome. Nature. 2012; 488:116–120. [PubMed: 22763441]
27. Mouse EC, et al. An encyclopedia of mouse DNA elements (Mouse ENCODE). Genome biology. 2012; 13:418. [PubMed: 22889292]
28. Crawford GE, et al. Genome-wide mapping of DNase hypersensitive sites using massively parallel signature sequencing (MPSS). Genome research. 2006; 16:123–131. [PubMed: 16344561]
29. Nord AS, et al. Rapid and pervasive changes in genome-wide enhancer usage during mammalian development. Cell. 2013; 155:1521–1531. [PubMed: 24360275]
30. Bailey TL, et al. MEME SUITE: tools for motif discovery and searching. Nucleic acids research. 2009; 37:W202–W208. [PubMed: 19458158]
31. Gerstein MB, et al. Architecture of the human regulatory network derived from ENCODE data. Nature. 2012; 489:91–100. [PubMed: 22955619]
32. Fleischmann A, et al. Fra-1 replaces c-Fos-dependent functions in mice. Genes & development. 2000; 14:2695–2700. [PubMed: 11069886]
33. Kitano J, et al. Tamalin, a PDZ domain-containing protein, links a protein complex formation of group 1 metabotropic glutamate receptors and the guanine nucleotide exchange factor cytohesins.

The Journal of neuroscience : the official journal of the Society for Neuroscience. 2002; 22:1280–1289. [PubMed: 11850456]

34. Gu Y, et al. Obligatory Role for the Immediate Early Gene NARP in Critical Period Plasticity. Neuron. 2013; 79:335–346. [PubMed: 23889936]
35. Chang MC, et al. Narp regulates homeostatic scaling of excitatory synapses on parvalbumin-expressing interneurons. Nature neuroscience. 2010; 13:1090–1097.
36. Beck KD, Powell-Braxton L, Widmer HR, Valverde J, Hefti F. Igf1 gene disruption results in reduced brain size, CNS hypomyelination, and loss of hippocampal granule and striatal parvalbumin-containing neurons. Neuron. 1995; 14:717–730. [PubMed: 7718235]
37. Sugo N, et al. Nucleocytoplasmic translocation of HDAC9 regulates gene expression and dendritic growth in developing cortical neurons. The European journal of neuroscience. 2010; 31:1521–1532. [PubMed: 20525066]
38. Ronan JL, Wu W, Crabtree GR. From neural development to cognition: unexpected roles for chromatin. Nature reviews. Genetics. 2013; 14:347–359.
39. Zhou Z, et al. Brain-specific phosphorylation of MeCP2 regulates activity-dependent Bdnf transcription, dendritic growth, and spine maturation. Neuron. 2006; 52:255–269. [PubMed: 17046689]
40. Li H, Durbin R. Fast and accurate short read alignment with Burrows-Wheeler transform. Bioinformatics. 2009; 25:1754–1760. [PubMed: 19451168]
41. Zhang Y, et al. Model-based analysis of ChIP-Seq (MACS). Genome biology. 2008; 9:R137. [PubMed: 18798982]
42. Rupp RA, Snider L, Weintraub H. Xenopus embryos regulate the nuclear localization of XMyoD. Genes & development. 1994; 8:1311–1323. [PubMed: 7926732]
43. Heckman KL, Pease LR. Gene splicing and mutagenesis by PCR-driven overlap extension. Nature protocols. 2007; 2:924–932.
44. Heinz S, et al. Simple combinations of lineage-determining transcription factors prime cis-regulatory elements required for macrophage and B cell identities. Molecular cell. 2010; 38:576–589. [PubMed: 20513432]

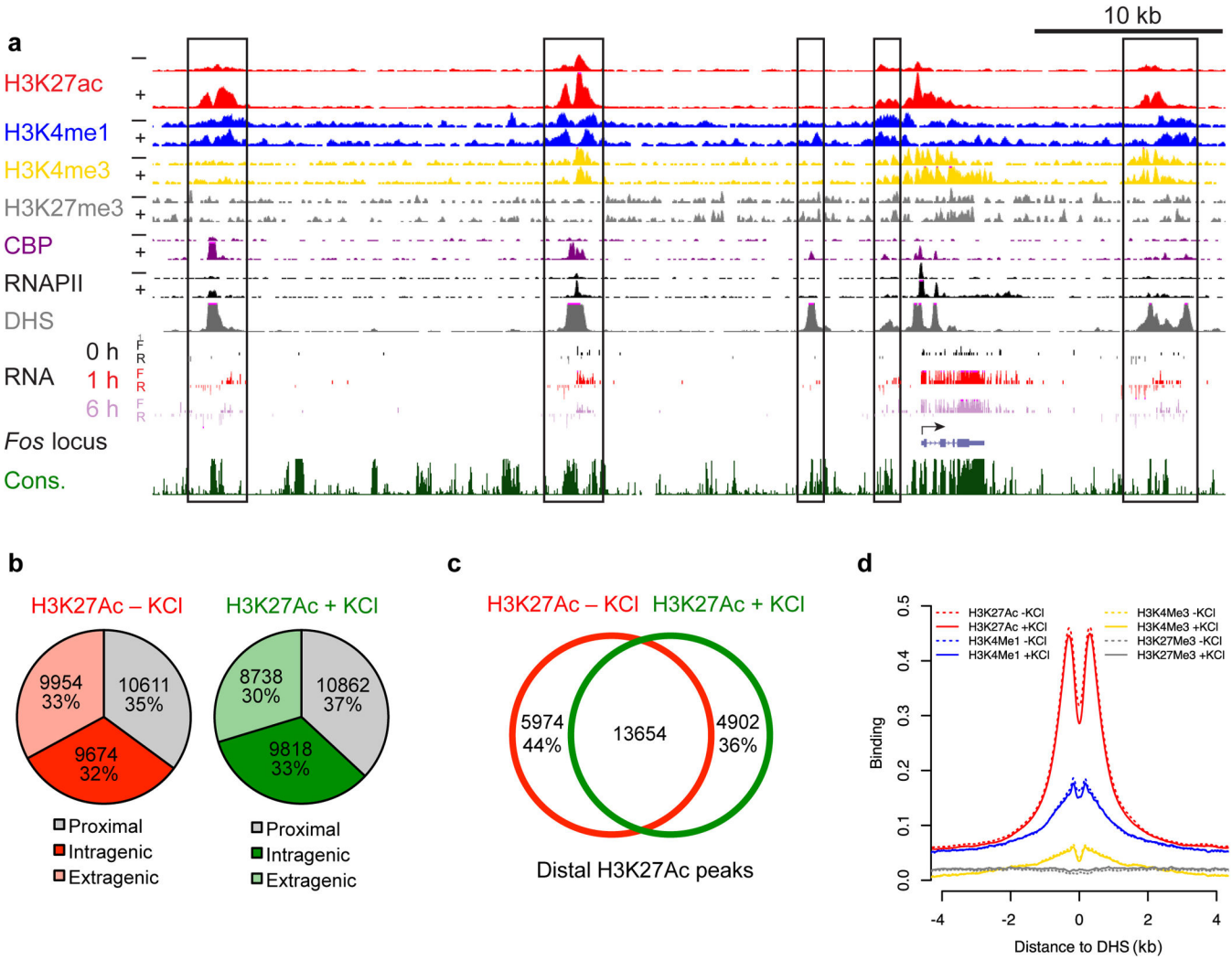

Figure 1. Genome-wide analysis of H3K27ac ChIP-seq peaks

a) UCSC genome browser tracks of the *Fos* locus with data for indicated histone modifications and DNaseI hypersensitivity mapping from p56 mouse cortex (generated by the Mouse ENCODE project[27]). H3K4me1, H3K4me3, H3K27me3 RNA Pol II, CBP and RNA-seq tracks were generated previously[18].

b) Genomic distribution of H3K27ac peaks before and after membrane depolarization. Peaks +/− 1 kb of a TSS are listed as proximal.

c) Overlap of gene distal (> 1 kb from a TSS) H3K27ac peaks before and after membrane depolarization

d) Aggregate plot of H3K4me1, H3K4me3, H3K27ac and H3K27me3 signal before and after membrane depolarization centered at gene-distal DHS sites enriched for H3K27ac.

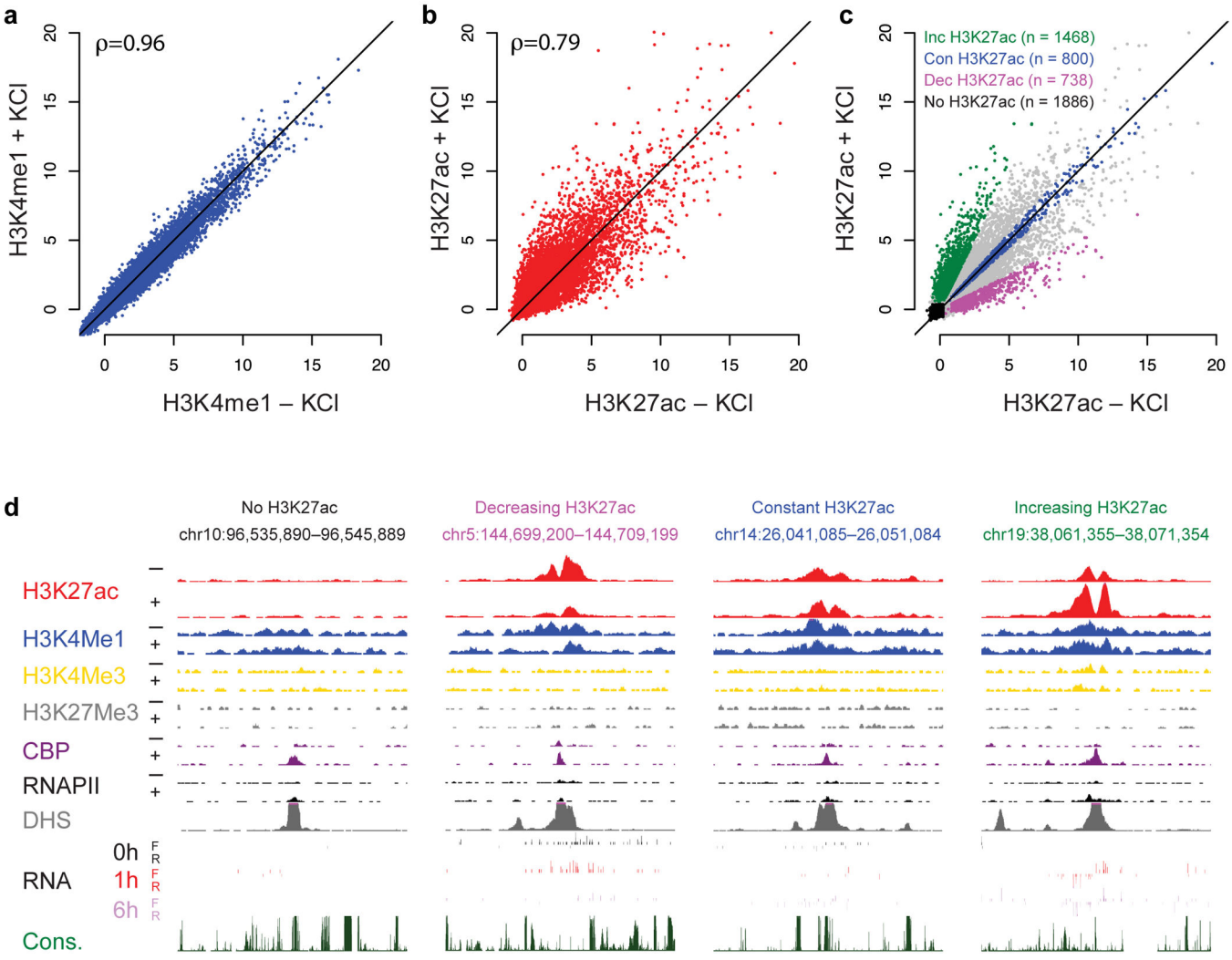

Figure 2. H3K27ac dynamics at activity-regulated enhancers

a) H3K4me1 ChIP-seq signal at CBP/H3K4me1-enriched sites before and after 2 h membrane depolarization by KCl (ρ= 0.96, Spearman's rank correlation coefficient).

b) H3K27ac ChIP-seq signal at CBP/H3K4me1-enriched sites before and after 2 h membrane depolarization by KCl (ρ = 0.79, Spearman's rank correlation coefficient).

c) Classification of putative activity-regulated enhancers by distinct H3K27ac dynamics in response to neuronal activity (see methods).

d) Representative loci demonstrating distinct H3K27ac dynamics at enhancers in response to neuronal activity.

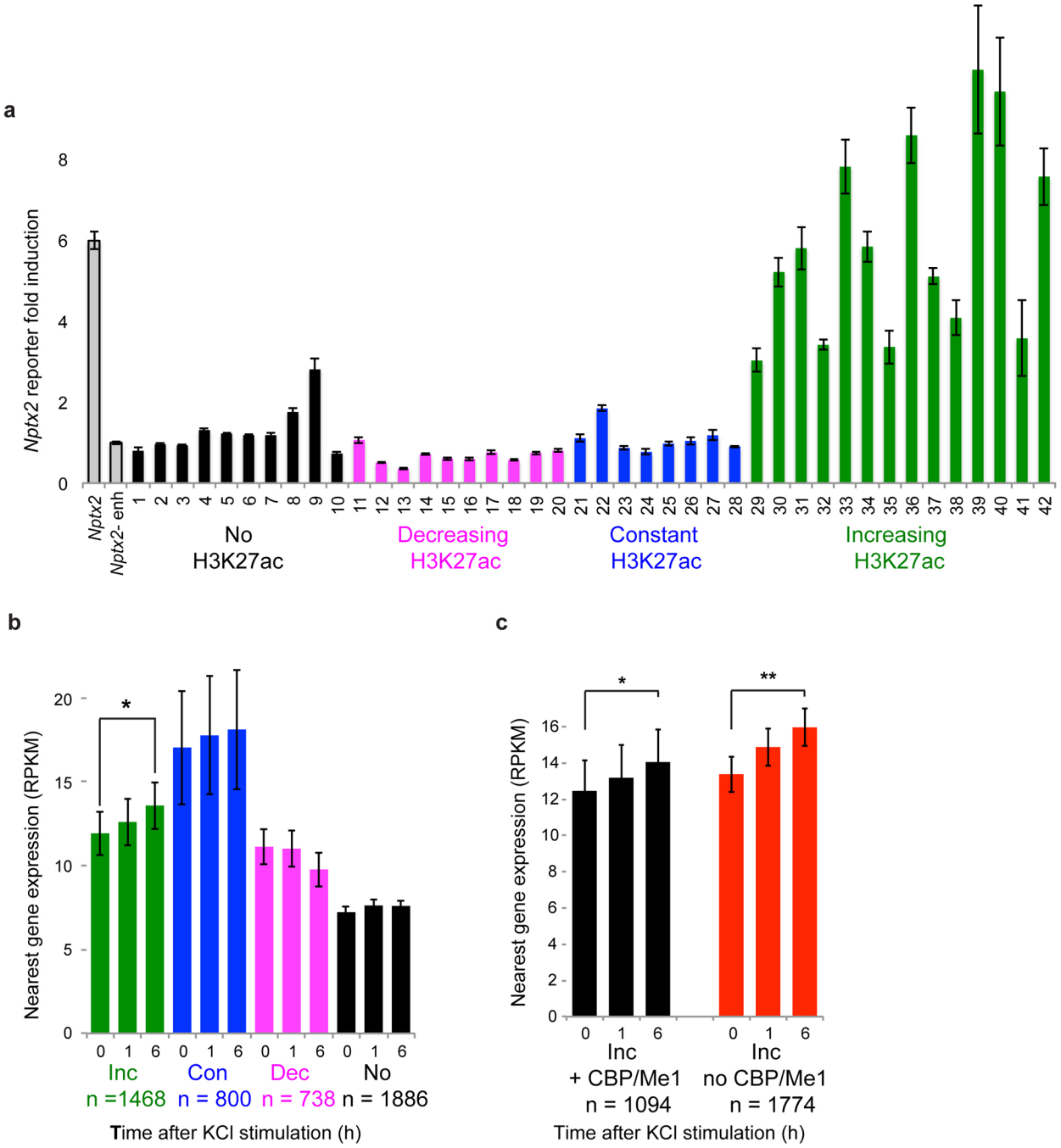

Figure 3. Functional analysis of enhancers with distinct H3K27ac dynamics

a) Functional testing of enhancers from distinct H3K27ac classes in cultured DIV7 cortical neurons. All results are displayed as a fold-increase over the *Nptx2* reporter backbone without the *Nptx2* enhancer element. Error bars represent standard error of the mean (S.E.M.) from 3 biological replicates with 3 technical replicates for each experiment.

b) Average expression of the nearest gene to elements from each class (measured by RNA-seq; RPKM = reads/kb mapped). Gene expression analysis was performed following 0,1,or 6 h of membrane depolarization by KCl (generated by Kim et al.[18]). *p = 7.83×10^{-11}; paired

Wilcoxon signed rank test. The number of genes in each group is indicated below the x-axis. Error bars represent standard S.E.M.

c) Average expression of the nearest gene to enhancers with increasing H3K27ac with and without CBP/H3K4me1 enrichment (*$p = 3.21e^{-08}$,**$p < 2.2e^{-}16$). Error bars represent S.E.M.

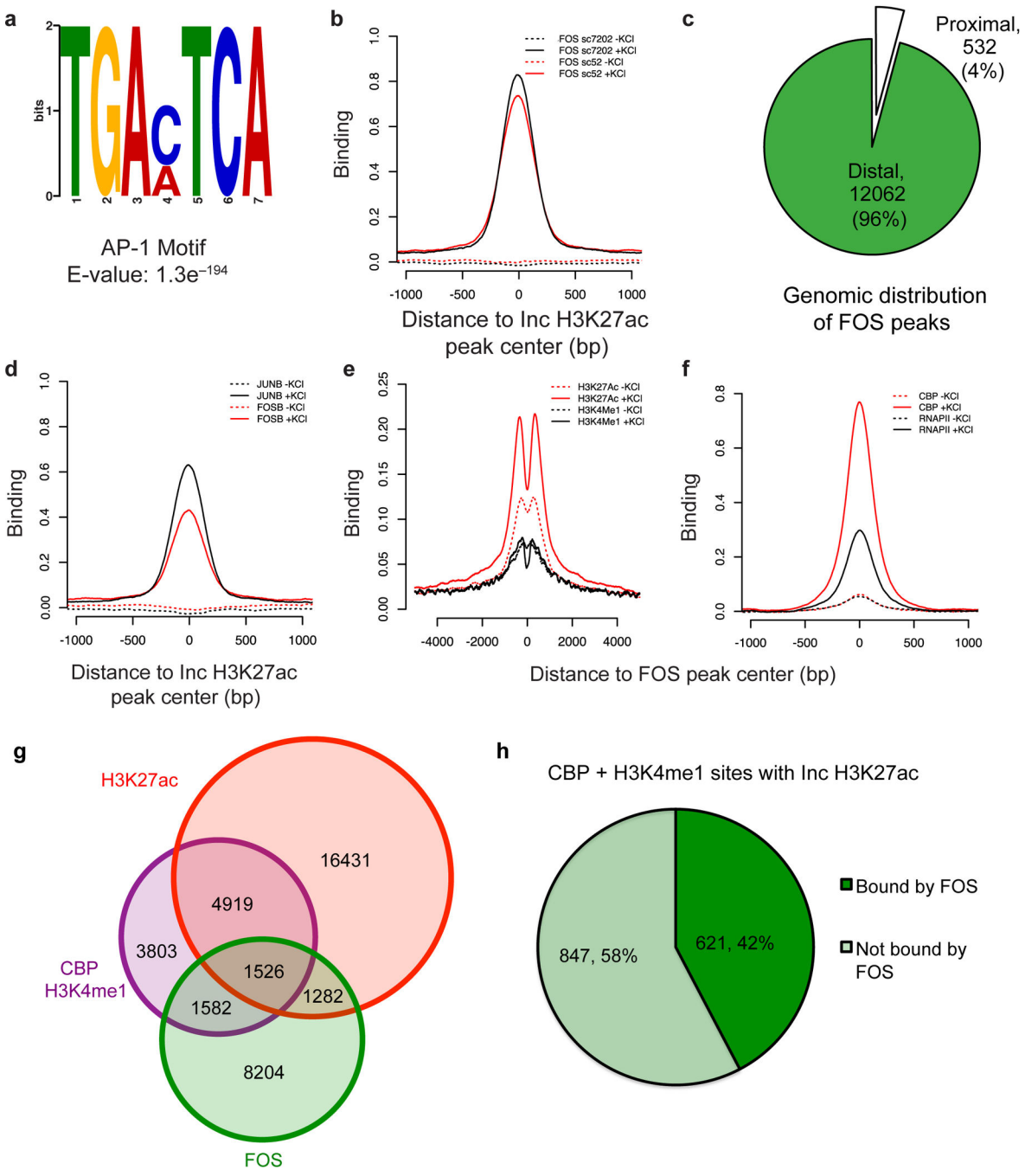

Figure 4. FOS binding is highly enriched at neuronal activity-regulated enhancers

a) Position weight matrix of the AP-1 site identified by MEME *de novo* motif search, performed with a search window of 150 bp from the center of the CBP peak within each activity-regulated enhancer.

b) Aggregate plots of ChIP-seq signal for FOS at activity-regulated enhancers. Signal from a ChIP-seq experiment performed with an additional FOS antibody (sc-7202) also indicated.

c) Distribution of FOS peaks with respect to gene TSS. Distal binding sites were defined as > 1 kb from an NCBI annotated RefSeq TSS.

d) Aggregate plots of FOSB and JUNB binding at activity-regulated enhancers
e) Aggregate plot of ChIP-seq signal for H3K4me1 and H3K27ac before and after membrane depolarization at FOS binding sites genome-wide.
f) Aggregate plot of CBP binding and RNA PolII binding before and after membrane depolarization at FOS binding sites genome-wide.
g) Genome-wide overlap between H3K27ac peaks, CBP/H3K4me1-enriched sites, and FOS peaks throughout the genome.
h) Fraction of increasing H3K27ac peaks bound by FOS

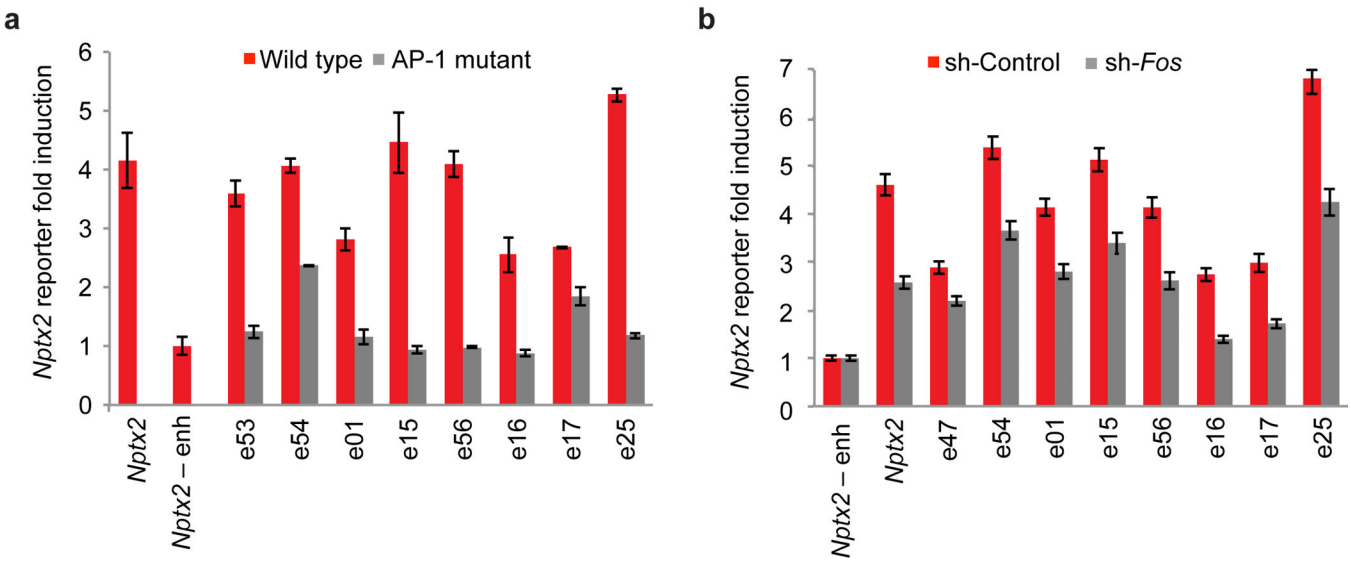

Figure 5. AP-1 transcription factors are required for proper function of activity-regulated enhancers

(a) Effect of AP-1 site mutation on FOS-bound, activity-dependent enhancer function in the *Nptx2* reporter. AP-1 mutant enhancers have a single point mutation introduced into every AP-1 site within the enhancer that abrogates AP-1 complex binding.

(b) Effect of *Fos* shRNA co-transfection on activity-regulated enhancer activity compared to a control shRNA plasmid (see methods). Error bars for each panel represent S.E.M for 3 biological replicates with 3 technical replicates for each experiment.

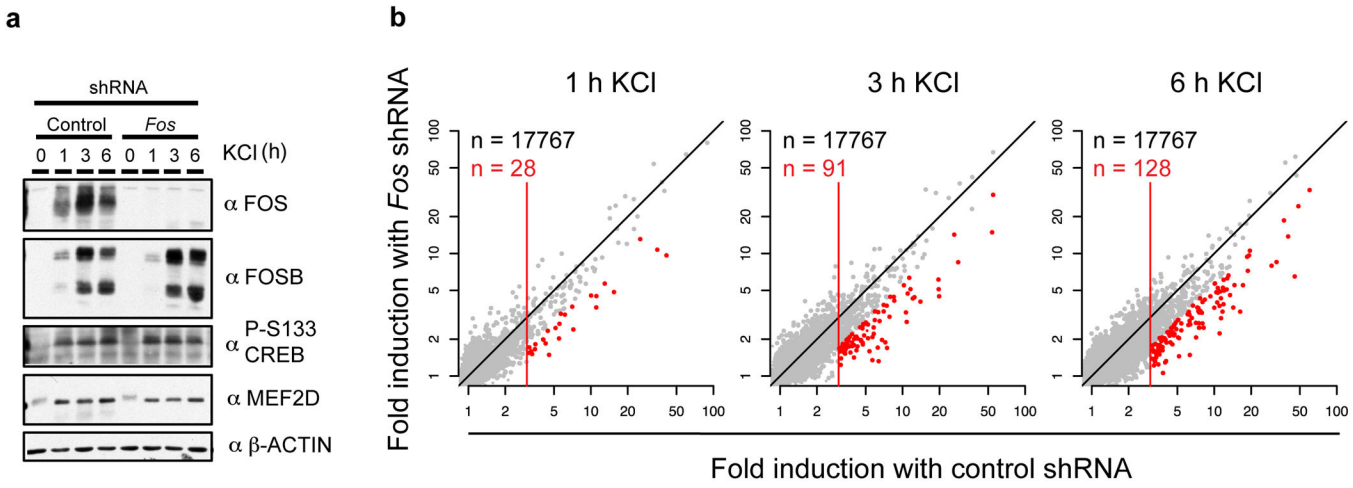

Figure 6. FOS activates an extensive gene program in neurons that regulates synaptic development and function

(**a**) Western blot for FOS, FOSB and proteins involved in activity-regulated signaling from cells expressing either control or *Fos* shRNA after 0,1,3, or 6 h of KCl stimulation. (**b**) Quantification of gene expression changes in cells expressing a lentiviral shRNA construct targeting FOS compared to a control shRNA targeting firefly luciferase. Neurons were treated with KCl for the indicated times (0,1,3,6 h) and gene expression was measured by microarray from biological replicate samples (n = 2 for each condition). The line indicates genes whose expression is induced by neuronal activity at least 3-fold at each of the 3 timepoints in the control condition. Red dots indicate activity-regulated microarray probes whose expression was reduced by at least 1.5-fold in the FOS shRNA condition compared to control shRNA. The number of total probesets at each timepoint and the activity-induced probes with 1.5-fold decreased expression in the *Fos* shRNA condition are listed on each scatterplot.

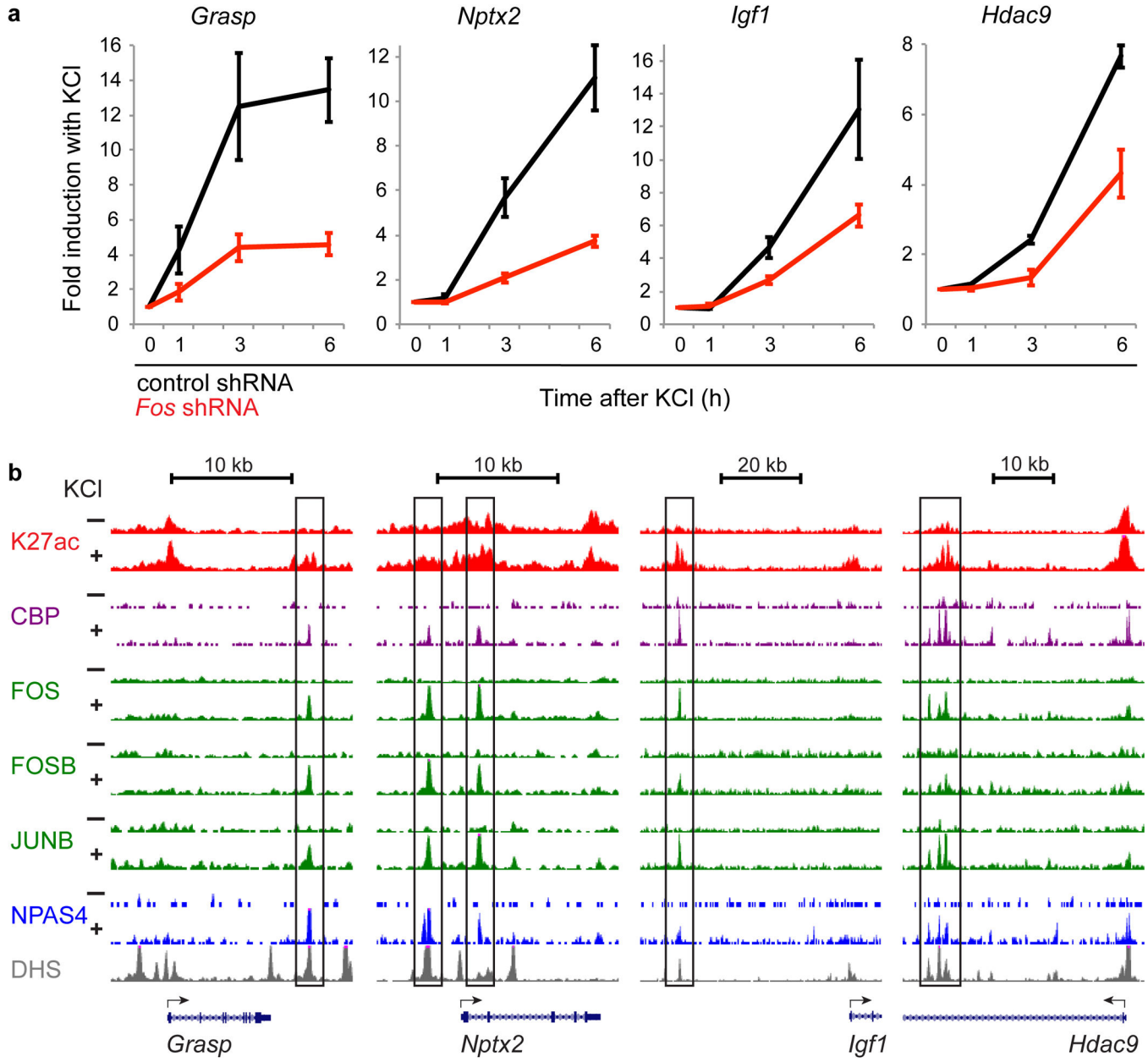

Figure 7. Integrated genomic analysis identifies direct targets of FOS

(a) Expression values measured by microarray of selected direct FOS target genes at each timepoint of KCl stimulation (error bars indicate S.E.M., n = 2)

(b) Genome browser tracks for each locus shown in (a) indicating enhancer associated features and AP-1 transcription factor binding data. Putative enhancer elements are indicated by the boxed regions. Npas4 ChIP-seq data was generated previously[18].

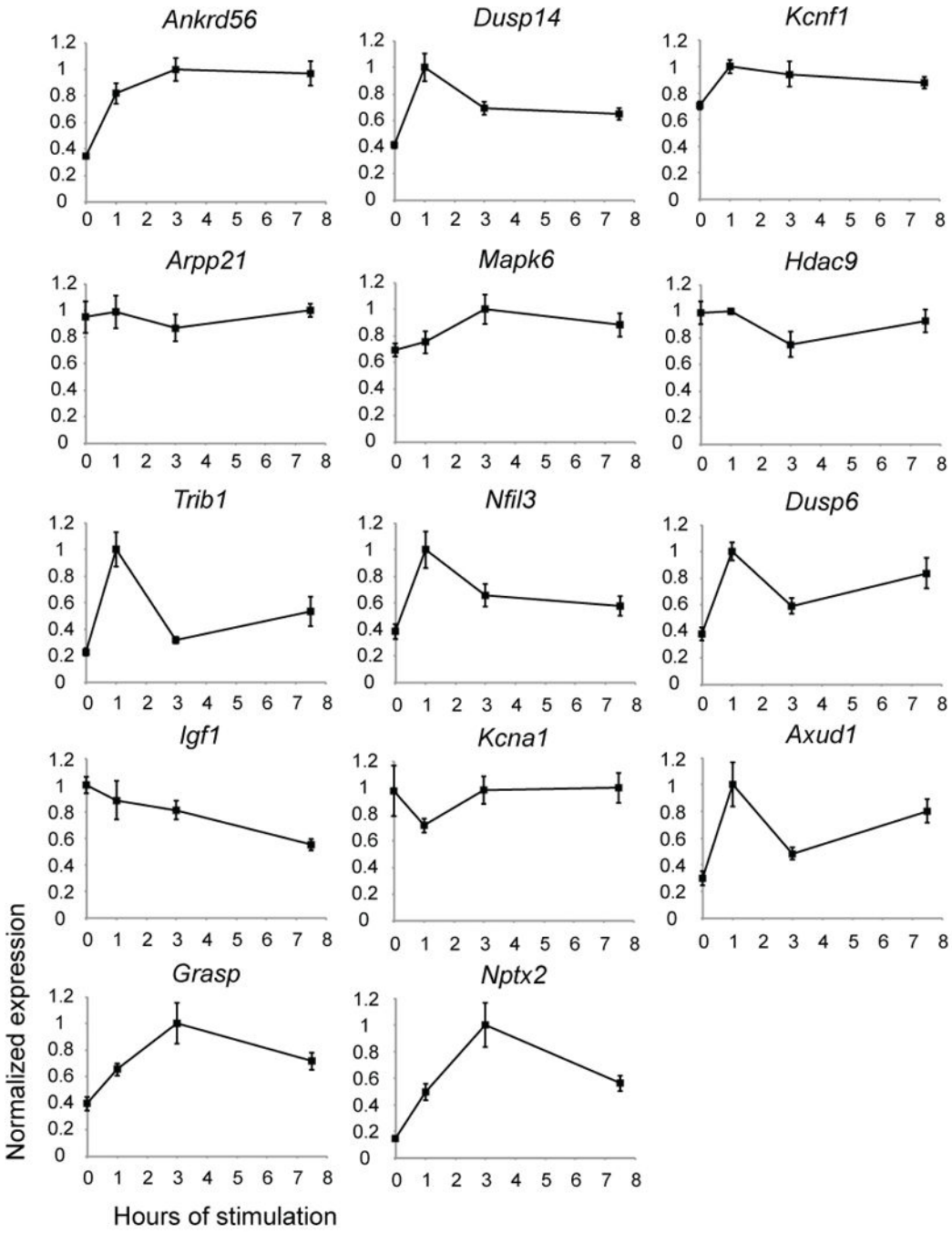

Figure 8. Expression of FOS direct target genes in mouse visual cortex

The expression of each indicated direct FOS target gene in the primary visual cortex was measured by qRT-PCR. Seven week-old mice were dark housed for one week and exposed to light for the indicated time periods. Measured expression levels for each gene were normalized to the timepoint with the highest level of expression. Error bars indicate S.E.M. from 4 animals.